Protein Science (2000), *9*:361–368. Cambridge University Press. Printed in the USA.

Role of the switch II region in the conformational transition of activation of Ha-*ras*-p21

JOSÉ FERNANDO DÍAZ,[1] MARÍA MILAGROSA ESCALONA,[2] STEVEN KUPPENS, AND YVES ENGELBORGHS

Laboratory of Biomolecular Dynamics, Katholieke Universiteit Leuven, Celestijnenlaan 200D, B-3001, Heverlee, Belgium

(RECEIVED July 19, 1999; FINAL REVISION November 5, 1999; ACCEPTED November 9, 1999)

Abstract

The role of the switch II region in the conformational transition of activation of Ha-*ras*-p21 has been investigated by mutating residues predicted to act as hinges for the conformational transition of this loop (Ala59, Gly60, and Gly75) (Diaz JF, Wroblowski B, Schlitter J, Engelborghs Y, 1997, *Proteins 28*:434–451), as well as mutating the catalytic residue Gln61. The proposed mutations of the hinge residues decrease the rate of the conformational transition of activation as measured by the binding of BeF_3^- to the GDP-p21 complex. Also, the thermodynamic parameters of the binding reaction are altered by a factor between three and five, depending on the temperature. (Due to changes in activation and reaction enthalpies, partially compensated by entropy changes.) The control mutation Q61H in which only the catalytic residue is changed has only a limited effect on the kinetic rate constants of the conformational transition and on the thermodynamic parameters of the reaction.

The fact that mutations of the hinge residues of the switch II region affect both the binding of the phosphate analog and the conformational transition of activation indicates that the switch II is implicated both in the early and the late states of the transition.

Keywords: conformational change; G-proteins; molecular dynamics; molecular switch; stopped flow

Ten years ago the structure of Ha-*ras*-p21, a protein (189 residues) that is a member of the group of the small guanine binding proteins (G-proteins), was determined by Tong et al. (1989). The high resolution three-dimensional (3D) structures of the active and inactive forms of Ha-*ras*-p21 were published subsequently (Pai et al., 1990; Tong et al., 1991). A quick comparison between both structures shows that there are two molecular switches at the surface of the molecule, whose structural state is controlled by the binding state of the molecule. The Ha-*ras*-p21 molecule binds guanine nucleotides complexed with magnesium ions. The physiological state of the protein depends on the nature of the bound nucleotide, as it is activated by the interchange of bound GDP with GTP and deactivated by the hydrolysis of bound GTP. Both of these processes (hydrolysis and nucleotide exchange) determine the conformational state of the protein and are controlled by external proteins: the GTPase activating proteins (GAPs) in the case of the hydrolysis (Adari et al., 1988) and the guanine exchange factors (GEFs) and guanine release proteins (GNRPs) in the case of the nucleotide exchange (McCormick, 1994).

In addition to the clinical interest of the system (point mutations of the *ras*-genes can be found in 30% of the human tumors (Barbacid, 1987)), the system is of interest for us, as G-proteins are the paradigm of a molecular switch. The structures of the G-proteins and the biology of their activation are widely studied (for a review, see Sprang, 1997). Much is known about how *ras*-p21 transmits the signal it receives form the surface of the cell to the cascade of kinases. Nevertheless, very little is known about the internal mechanisms of activation: how is the signal transmitted from the nucleotide binding site to both molecular switches, enabling in this way signal transmission downstream? In addition, we consider the structure of *ras*-p21 as a kind of model for GTP-activated proteins. It is reflected in two other GTP-depending proteins with no sequence homology with it: tubulin and FtsZ (Löwe & Amos, 1998; Nogales et al., 1998). The biological relevance of the system as well as the small size of the molecule make it a perfect model system to study the mechanisms of conformational transition in GTP-activated proteins.

Reprint requests to: Yves Engelborghs, Laboratory of Biomolecular Dynamics, Katholieke Universiteit Leuven, Celestijnenlaan 200D, B-3001, Heverlee, Belgium; e-mail: yves.engelborghs@fys.kuleuven.ac.be.

[1]Present address: Centro de Investigaciones Biológicas, Consejo Superior de Investigaciones Científicas, C/O Velazquez 144, 28006 Madrid, Spain.

[2]Present address: Servicio de Reumatología, Hospital General Universitario Gregorio Marañón, C/O Dr. Esquerdo 46, 28009, Madrid, Spain.

Abbreviations: GDP, 5′-guanosine diphosphate; GTP, 5′-guanosine triphosphate; GAPs, GTPase activating proteins; GEFs, guanine exchange factors; GNRPs, guanine release proteins; MD, molecular dynamics; TMD, targeted molecular dynamics; DTE, dithioerythritol; PCR, polymerase chain reaction; SDS-PAGE, sodium dodecyl sulfate-polyacryl amide gel electrophoresis.

Studying the dynamics of a conformational transition is not an easy task. Structure analysis techniques have either a high structural resolution but a limited time resolution (Laue diffraction methods) (Schlichting et al., 1990), or a good time resolution but poor structural resolution (stopped flow X-ray scattering) (Díaz et al., 1998). In this way, no detailed insights into the structures of the intermediates can be observed using direct structural techniques. We decided to use computational methods, i.e., molecular dynamics (MD) (Díaz et al., 1995) and Targeted molecular dynamics (TMD) (Schlitter et al., 1994; Díaz et al., 1997b), to find possible hinges and levers of the conformational transition, as well as to find a possible pathway for the activation and deactivation of the molecule. By using the TMD technique (Díaz et al., 1997b), we were able to model the pathway of activation and deactivation of Ha-*ras*-p21, as a series of successive conformational changes of certain residues and parts of the molecule with transient energy maxima during the transition. In this way it became clear that the conformational transition between both states of the protein is not a single process, but a succession of different micro transitions that complete the process as a chain reaction. It is possible to determine the residues that may constitute energy barriers for a certain micro transition and then design mutants that may stabilize or destabilize the transition state of that particular micro transition.

The pathway of activation of *ras*-p21 is started by the introduction of the γ-phosphate in its binding site. According to the modeling done by Díaz et al. (1997b), there is enough space in the nucleotide binding cup of the GDP-bound conformation to accommodate the γ-phosphate. The presence of the phosphate destabilizes the conformation of the P-loop that transmits the signal to the effector loop and the switch II region. All these processes involve several movements and internal rearrangements of the conformation of the loops, which involve dihedral transitions in certain residues that can be associated with energy barriers. By mutating these residues it should in principle be possible to increase or decrease the energy barriers and so to accelerate or decelerate the conformational transition or to stabilize or destabilize one of the conformational states.

An experimental model of the conformational transition had to be developed to validate the calculation method and the model. The problem is that in physiological conditions the rate limiting step of the conformational transition of activation is not the transition itself but the hydrolysis of the γ-phosphate in the case of the deactivation and the interchange of the nucleotide in the case of the activation (Adari et al., 1988; Krengel et al., 1990; Neal et al., 1990; Antonny et al., 1991; Lowy & Willumsen, 1993; Moore et al., 1993). The obvious solution to this problem is the use of a phosphate analogue that would be able to reversibly bind or dissociate from its site, thus activating or deactivating the protein without the steps of hydrolysis or nucleotide exchange (Bigay et al., 1987). Despite the early reports of the inability of phosphate analogues to activate *ras*-like proteins (Kahn, 1991), we have demonstrated (Díaz et al., 1997a) using an active mutant of Ha-*ras*-p21 (Y32W) that contains a fluorescent label at the effector loop, that beryllium trifluoride is able to bind to the γ-phosphate site with a millimolar dissociation constant (K_d = 8.13 mM at 25 °C), and to induce the conformational transition toward a GTP-like state. Using the binding reaction of BeF_3^- to the Ha-*ras*-p21, it is possible to monitor the levels of the conformational transition. By mutating the positions that are supposed to be involved in the conformational transition, and monitoring the kinetics of the binding reaction of the phosphate analogues to the mutants, we should be able to confirm our predictions and add support to the modeling system employed.

Most of the residues shown to act as hinges of the conformational transition are at the sides of the three main areas implicated in the switching. Most of them are small residues Gly12, Gly13, Gly48, Ala59, Gly60, Gly75, except those at both sides of the effector loop, Val29 and Ile36. The experimental data concerning these mutants show that the naturally occurring mutations at positions 12, 13, 59, and 61 result in proteins with transforming properties (Barbacid, 1987), while mutations at position 60 (Sung et al., 1995) block the conformational transition.

The contribution of the effector loop to the conformational transition was studied previously (Kuppens et al., 1999). In that work, the V29G and I36G mutants were constructed since these residues were the only large ones predicted to act as hinges of the conformational transition. Their mutation into glycines facilitates the conformational transition of the effector loop. The results show that those residues are effectively involved in the conformational transition, and the reduction of the size of their side chains removes energetic barriers accelerating the rate of the conformational transition by two orders of magnitude.

In the present study, we have investigated the role of the hinge residues of the switch II region. As the residues at both sides of the area are small, we hope that replacement with bigger residues at this positions might introduce additional energetic barriers and slow down the transition. A mutant in the catalytic residue Q61H was constructed as a control mutant. This mutant is oncogenic because the GTPase activity is almost abolished but the conformational transition between both states should not be affected by the mutation.

Results

Equilibrium of binding of BeF_3^- to the double mutants

We have characterized the binding equilibrium of BeF_3^- to its site in GDP-bound Y32W-Ha-*ras*-p21 using the change in fluorescence of Trp32 upon binding. The equilibrium was measured at different temperatures so that a thermodynamical characterization of the binding reaction could be made. The reaction was found to be very fast, as previously described (Díaz et al., 1997a; Kuppens et al., 1999), and was completed within the mixing time. Figure 1 shows the titration curve of GDP-p21(Y32W-Q61H) at 25 °C. The curves were fitted to Equation 1, derived directly from the mass balance, the definition of the binding constant, and the specific fluorescence intensity:

$$F_x = \frac{F_0 + F_1 \cdot [BeF_3^-] \cdot K_{app}}{1 + [BeF_3^-] \cdot K_{app}} \quad (1)$$

where F_x is the measured fluorescence intensity at a given concentration of beryllium trifluoride, F_0 the specific fluorescence intensity of the GDP-bound form, F_1 the specific fluorescence intensity of the (BeF_3^--GDP)-bound form, and K_{app} the apparent binding constant. (Apparent because it could be a function of other parameters, e.g., pH, etc.) Similar curves were obtained for the other mutants. Previously we have done extensive control experiments to show that the reduction of the fluorescence intensity is not due to a general quenching effect by any of the components present (Díaz et al., 1997a).

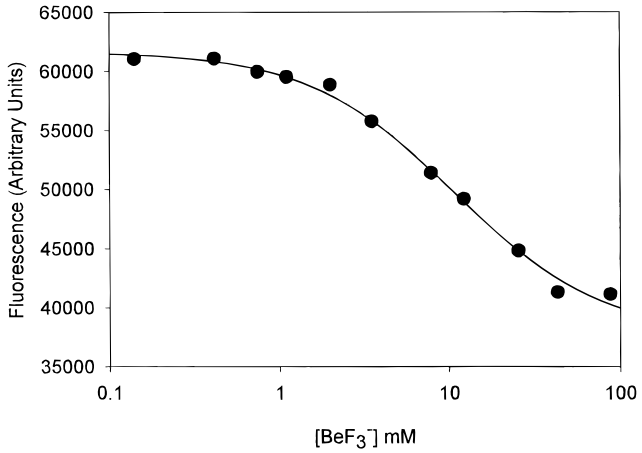

Fig. 1. Titration curve of 10 μM GDP-Ha-*ras*-p21(Y32W-Q61H) with BeF_3^- at 25 °C. The filled circles are the experimental data points; the solid line is the fitting to Equation 1. The symbols are larger than the error bars.

Figure 2 shows the van't Hoff representation of the binding constants of BeF_3^- to the different double mutants of GDP-Ha-*ras*-p21. The apparent binding constants and thermodynamic parameters obtained are listed in Table 1 and agree within experimental error with the kinetically determined constants (Table 2). The reaction is endothermic for three of the double mutants, and athermic for the Y32W-G75V mutant, and in all cases it is entropy driven. The binding constants determined are similar to those described for the Y32W mutant except for the Y32W-G75V mutant whose affinity is reduced.

Kinetics of binding of BeF_3^- to Ha-ras-p21 altered in the hinges of the switch II region

The kinetics of binding of BeF_3^- to all mutants studied were found to be very fast and so they were measured using stopped flow techniques as described in Díaz et al. (1997a). Figure 3 shows the kinetics of the binding reaction of the Y32W-Q61H mutant to the ligand. The kinetic curves for all the mutants have to be expressed as a sum of two exponentials like those obtained for the reference mutant Y32W (Díaz et al., 1997a). This is in contrast with the single exponential behavior of the fluorescence decay of Trp32 upon binding of the ligand to the "fast" mutants V29G-Y32W and Y32W-I36G (Kuppens et al., 1999).

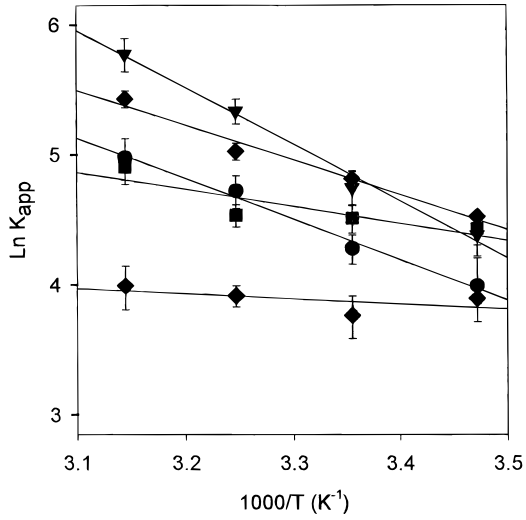

Fig. 2. van't Hoff representation of the binding constants of BeF_3^- for the mutants of Ha-*ras*-p21. Data for: Y32W-G60A (triangles), Y32W (upper diamonds), Y32W-A59T (circles), Y32W-Q61H (squares), Y32W-G75V (lower diamonds).

The time scale of the curves is increased by a factor of three to five for the mutants Y32W-A59T, Y32W-G60A, and Y32W-G75V, but is almost unaffected for Y32W-Q61H. The effect is, therefore, not so spectacular as the acceleration observed for the V29G-Y32W and Y32W-I36G mutants (Kuppens et al., 1999).

The dependence of the observed rate constant on the concentration of the ligands is in all cases linear for the fast process and hyperbolic for the slow process. Figure 4 shows the dependence on the concentration of the analog, of the observed rate constants of binding to one of the mutants (Y32W-Q61H). This can only be explained by a mechanism consisting of two consecutive steps: i.e., a first bimolecular step of binding followed by a slower step of conformational isomerization of the initial complex, as previously described (Díaz et al., 1997a):

$$\text{GDP-p21} + BeF_3^- \underset{k_{-1}}{\overset{k_{+1}}{\rightleftarrows}} (\text{GDP-}BeF_3^-)\text{-p21} \underset{k_{-2}}{\overset{k_{+2}}{\rightleftarrows}} (\text{GDP-}BeF_3^-)\text{-p21*}. \quad (2)$$

Such a model leads to a linear concentration dependence for the fast step:

$$k_{1,\,obs} = k_{+1}\cdot[BeF_3^-] + k_{-1} \quad (3)$$

and to a hyperbolic relation for the slow step:

$$k_{2,\,obs} = \frac{k_{+2}\cdot K_1\cdot[BeF_3^-]}{1 + K_1\cdot[BeF_3^-]} + k_{-2}. \quad (4)$$

An alternative explanation for two exponentials would be two parallel pathways. This would imply an heterogeneity of the protein for which there is no evidence at all. Moreover, the K_1 determined from the fitting of $k_{2,obs}$ to Equation 4 agrees with the K_1 obtained from the fitting of $k_{1,obs}$ (Equation 3).

Table 2 summarizes the kinetic constants determined by the global analysis of all kinetic data for the four mutants studied. It can be noticed that while the first step of the binding reaction itself is only very weakly affected by the mutations, the k_{+2} constant is heavily reduced in the mutants in which the residue at the predicted hinge has been replaced by a bigger group. In contrast, the kinetics are only marginally affected when the catalytic residue is altered.

Thermodynamic parameters of the binding of BeF_3^- to the switch II Ha-ras-p21 mutants

The kinetic and equilibrium constants being determined at different temperatures (Tables 1, 2), it is possible to obtain the thermodynamic parameters and the activation energies of the individual steps of the reaction. Table 3 shows the activation energy and preexponential factors of the individual kinetic reactions. Table 4

Table 1. *Equilibrium constants and thermodynamic parameters of binding of BeF_3^- to the double mutants of Ha-ras-p21*

	Y32W[a]	Y32W-A59T	Y32W-G60A	Y32W-Q61H	Y32W-G75V
K_{app} 15 °C (M^{-1})	92 ± 3	54 ± 13	80 ± 12	84 ± 10	49 ± 2
K_{app} 25 °C (M^{-1})	123 ± 8	72 ± 8	115 ± 10	91 ± 10	43 ± 2
K_{app} 35 °C (M^{-1})	152 ± 10	112 ± 14	208 ± 20	93 ± 8	50 ± 4
K_{app} 45 °C (M^{-1})	211 ± 15	145 ± 23	322 ± 41	135 ± 17	54 ± 9
ΔH_{app} (kJ mol^{-1})	22 ± 2	25 ± 2	36 ± 3	11 ± 4	3 ± 3
ΔS_{app} (J mol^{-1} K^{-1})	109 ± 5	123 ± 2	162 ± 2	75 ± 2	43 ± 2

[a]Data from Díaz et al. (1997a).

shows the enthalpy and entropy changes of the reaction steps. An enthalpic and entropic pathway can then be described (Figs. 5, 6).

Discussion

In our previous papers (Díaz et al., 1995, 1997a, 1997b), both structural and kinetic pathways of the activation reaction of Ha-*ras*-p21 were proposed. According to the calculated pathway, a series of concerted movements of the loops that change conformation transmit the recognition signal from the nucleotide binding site to the effector loop and the switch II region. These rearrangements of the loops that move as rigid bodies use certain residues as hinges. These residues undergo conformational transitions that can be monitored (see Fig. 7 of Díaz et al., 1997b) and correlated to the peaks that can be observed in the energy profile of the simulated transition (see Fig. 2 of Díaz et al., 1997b). The energy curves are, however, noisy and difficult to assign, but at least about five pronounced energy maxima are visible: a first broad one centered around 50 ps then three sharp ones centered around 90, 110, and 130 ps and a final one centered around 190 ps.

Table 2. *Results of the global kinetic analysis of binding of BeF_3^- to the double mutants studied*

		Y32W[a]	Y32W-A59T	Y32W-G60A	Y32W-Q61H	Y32W-G75V
15°C	k_1	68.4 ± 0.4	108.5 ± 1.4	108.4 ± 0.3	67.2 ± 0.2	27.3 ± 0.1
	k_{-1}	2.73 ± 0.13	3.87 ± 0.29	2.04 ± 0.03	2.29 ± 0.02	1.08 ± 0.01
	K_1	25.0 ± 1.4	28.0 ± 1.7	53.1 ± 0.9	29.3 ± 0.4	25.3 ± 0.3
	k_2	1.98 ± 0.09	0.98 ± 0.36	0.93 ± 0.03	1.20 ± 0.01	0.65 ± 0.02
	k_{-2}	0.76 ± 0.07	1.93 ± 0.02	1.17 ± 0.02	0.64 ± 0.03	0.70 ± 0.01
	K_2	2.6 ± 0.4	0.5 ± 0.2	0.79 ± 0.04	1.87 ± 0.11	0.93 ± 0.05
	K_{ovr}	90 ± 7	42 ± 3	94 ± 4	84 ± 5	48 ± 3
25 °C	k_1	146 ± 2	159.3 ± 0.5	226.9 ± 0.8	141.3 ± 0.5	66.3 ± 0.2
	k_{-1}	4.65 ± 0.11	3.90 ± 0.04	3.37 ± 0.04	4.67 ± 0.05	3.00 ± 0.03
	K_1	31.4 ± 1.2	40.9 ± 0.5	67.3 ± 1.0	30.3 ± 0.4	22.1 ± 0.3
	k_2	3.74 ± 0.15	1.58 ± 0.05	1.12 ± 0.06	2.37 ± 0.03	1.47 ± 0.03
	k_{-2}	1.38 ± 0.12	2.23 ± 0.03	1.52 ± 0.08	1.18 ± 0.05	1.52 ± 0.02
	K_2	2.71 ± 0.4	0.71 ± 0.03	0.74 ± 0.08	2.01 ± 0.11	0.97 ± 0.04
	K_{ovr}	113 ± 11	70 ± 2	117 ± 7	91 ± 5	44 ± 1
35 °C	k_1	405 ± 3	363 ± 1	526 ± 2	280 ± 1	165 ± 1
	k_{-1}	10.4 ± 0.4	5.46 ± 0.04	4.22 ± 0.06	8.31 ± 0.07	6.36 ± 0.06
	K_1	39.0 ± 1.8	66.4 ± 0.8	124.6 ± 2.4	33.7 ± 0.4	25.9 ± 0.5
	k_2	7.50 ± 0.2	1.62 ± 0.04	1.56 ± 0.07	3.80 ± 0.05	2.97 ± 0.05
	k_{-2}	2.86 ± 0.12	2.41 ± 0.03	2.04 ± 0.31	2.25 ± 0.01	3.29 ± 0.03
	K_2	2.61 ± 0.3	0.67 ± 0.03	0.76 ± 0.18	1.69 ± 0.03	0.90 ± 0.02
	K_{ovr}	140 ± 12	111 ± 4	219 ± 26	91 ± 1	49 ± 2
45 °C	k_1	879 ± 5	606 ± 5	1,191 ± 8	656 ± 4	458 ± 2
	k_{-1}	19.8 ± 0.6	8.9 ± 0.2	6.25 ± 0.09	14.36 ± 0.27	15.33 ± 0.11
	K_1	44.4 ± 1.2	68.1 ± 2.1	190.5 ± 4.1	45.7 ± 1.2	29.9 ± 0.4
	k_2	15.3 ± 0.4	3.28 ± 0.16	2.18 ± 0.04	9.17 ± 0.24	4.50 ± 0.11
	k_{-2}	4.06 ± 0.15	3.14 ± 0.08	2.72 ± 0.41	4.72 ± 0.05	5.07 ± 0.07
	K_2	3.76 ± 0.5	1.03 ± 0.09	0.80 ± 0.07	1.94 ± 0.08	0.89 ± 0.03
	K_{ovr}	211 ± 15	138 ± 10	342 ± 22	134 ± 8	56 ± 2

[a]Data from Díaz et al. (1997a).

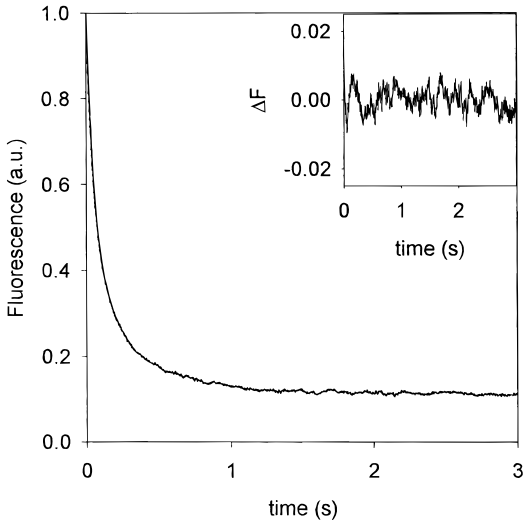

Fig. 3. Kinetics of binding for BeF_3^- to GDP-Ha-*ras*-p21 (Y32W-Q61H) at 25 °C. In the stopped-flow device 20 μM GDP-Ha-*ras*-p21 (Y32W-Q61H) is mixed with 87.7 mM BeF_3^- (final concentrations). The curve was fitted to a sum of two exponentials. Inset: the residuals of the fit. Similar curves are obtained for the other mutants.

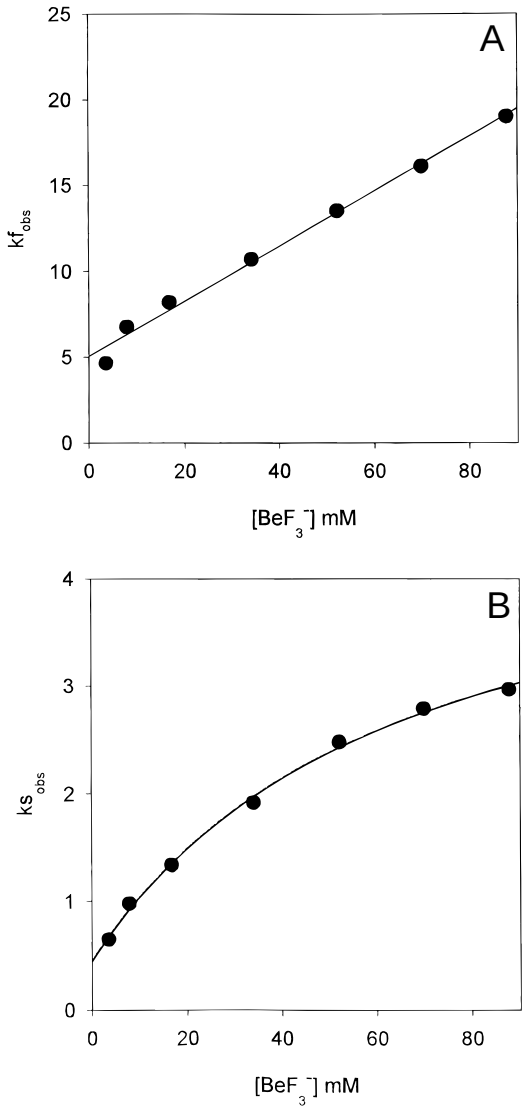

Fig. 4. Dependence on the concentration of BeF_3^- of the two observed rate constants at 25 °C for the binding reaction of the analog to GDP-Ha-*ras*-p21 (Y32W-Q61H). The continuous lines are the fits to a scheme of binding with conformational transition. Similar curves are obtained for the other mutants.

The process of the binding of the phosphate analog to Ha-*ras*-p21 (Díaz et al., 1997a) can be dissected in two steps: first, the bimolecular step of binding of the analog itself, and second, a monomolecular step of a conformational transition. The rate constant of the first bimolecular step (146 M^{-1} s^{-1} at 25 °C) is far too small to be attributed to a simple diffusion controlled binding step of a small ligand. The low value of this bimolecular step indicates that a conformational selection occurs during this initial step of binding.

In a previous paper (Kuppens et al., 1999), we designed two double mutants V29G-Y32W and Y32W-I36G at both sides of the effector loop. These residues were selected on the basis of the conformational transitions that are observed on the peptidic bonds in the DT pathway. Val29 and Ile36 were identified as the hinges of a segment (B) that shows many dihedral transitions. These residues were mutated with the intention of accelerating the reaction by decreasing the size of the hinge residues (so increasing their conformational freedom), and to study the role of the effector loop in the reaction of activation of Ha-*ras*-p21 induced by the binding of a phosphate analog. The two residues (and so the switch of the effector loop) are involved in both steps of the reaction; their mutations result in a large acceleration of both reaction steps and the activation energy of the conformational transition is largely reduced as expected. They also increase the enthalpy and the entropy of binding of the phosphate analog (in the first step), indicating that the mutations are affecting the binding site itself. Since, according to the predictions, the effector loop is involved in the early and late states of the transition, one can assume that the early states of the transition are involved in the first binding reaction.

Role of the catalytic residue on the activation pathway of Ha-ras-p21

Gln61 was selected to be mutated as it is the catalytic residue (Pai et al., 1990). Mutating it to a histidine abolishes the GTP-ase activity of Ha-*ras*-p21, resulting in a transforming protein (Krengel et al., 1990). No dihedral switch of this residue is observed during the calculated pathway so any mutation in this residue should not affect the conformational transition. The kinetic rates measured for this mutant are almost the same in all steps of the reaction as those of the reference mutant. This fact indicates that the catalytic residue plays no role in the conformational transition.

Role of switch II hinges in the activation pathway of Ha-ras-p21

To further dissect the transition into the observed steps and to investigate the role of the switch II region in the transition, three more double mutants were designed, constructed, and the kinetics of the conformational transition analyzed.

Table 3. *Activation energy and preexponential factors of BeF_3^- binding and conformational change reaction of switch II region of Ha-ras-p21*

	Y32W[a]	Y32W-A59T	Y32W-G60A	Y32W-Q61H	Y32W-G75V
Ea_{+1} (kJ mol^{-1})	67 ± 2	45 ± 5	61 ± 2	57 ± 3	71 ± 4
Ln (A_{+1})	32.4 ± 1.0	23.6 ± 1.9	30.1 ± 0.9	28.0 ± 1.1	33.0 ± 1.3
Ea_{-1} (kJ mol^{-1})	51 ± 2	21 ± 6	27 ± 2	46 ± 1	66 ± 5
Ln (A_{-1})	22.4 ± 1.3	10.1 ± 2.5	12.2 ± 1.0	20.2 ± 0.5	28.0 ± 1.9
Ea_{+2} (kJ mol^{-1})	52 ± 1	28 ± 7	22 ± 2	50 ± 3	50 ± 4
Ln (A_{+2})	22.3 ± 0.8	11.5 ± 2.7	9.0 ± 1.0	21.0 ± 1.0	20.4 ± 1.5
Ea_{-2} (kJ mol^{-1})	44 ± 4	12 ± 2	21 ± 1	50 ± 2	51 ± 4
Ln (A_{-2})	18.1 ± 1.4	5.5 ± 0.9	9.1 ± 0.3	20.6 ± 1.0	21.1 ± 1.4

[a]Data from Díaz et al. (1997a).

At one side of the loop Ala59 and Gly60 were mutated into threonine and alanine, respectively, the first is a classic oncogenic mutation (Barbacid, 1987), while the second is thought to affect the conformational transition of activation since it abolishes the activity of the mutant (Sung et al., 1995). The 58–59 and 59–60 peptidic bonds undergo dihedral switches at times coincident with energy maxima of the energy plot, i.e., about 98, 102, and 192 ps. Therefore, they should not influence the early stages of the transition (included in the first steps of binding), but the monomolecular reaction that accounts for the second step of the transition.

The results (Table 2; Figs. 5, 6) show that the kinetic rate constants of binding of BeF_3^- to GDP-Ha-*ras*-p21 are not much affected by the mutation. In the case of G60A, the thermodynamic parameters of the binding reaction are practically unaffected, while the A59T mutant has a reduced enthalpy of activation, the effect of which is compensated by a reduction of the activation entropy (related to the preexponential factor). Graphical analysis of the position of the threonine side chain in the A59T mutant generated using the WHATIF package (Vriend, 1990) indicates that the OH group of the side chain will point into the γ-phosphate site in the GDP conformation, while no influence of the Ala60 side chain is observed. Having an hydroxyl group pointing to the γ-phosphate position would provide an additional possible ligand for the fluorines of the analog, thus decreasing the activation enthalpy of the transition; however, the immobilization of the side chain should result in a decrease of the activation entropy that compensates the effect.

The intermediate state of the reaction is enthalpically destabilized by both mutations. However, this is compensated by a positive entropic effect, which results in a larger initial binding constant for these double mutants than for the reference mutant (Y32W). This could indicate that more interactions (e.g., with water) are broken in the initial state leading to a smaller ΔH^* but a larger ΔS^*.

The mutations have a reasonable effect on the second step of the conformational change. The k_{+2} kinetic constants are decreased by a factor ranging from three to five, depending on the temperature, as expected by the introduction of larger residues in the hinge group. This effect is mainly entropic, since the activation energy of the mutants is lower than that of the reference mutant, indicating that the newly introduced side chains contribute to the stabilization of the transition state. The loss of conformational freedom of the large side chains during the dihedral switch attributed to the transition state II is responsible for the effect on the kinetic rate.

In both cases, the end state is destabilized in comparison to the reference mutant, as the reaction is displaced toward the intermediate state. The origin of the destabilization is different, enthalpic in the case of the A59T mutant (according to the modeling done, the hydroxyl group of the threonine should no longer point to the γ-phosphate in the GTP-bound end state), and entropic in the case of the G60A mutant (perhaps due to a larger conformational restraint of the switch II region in the end state).

The results of the analysis of the Y32W-G60A mutant confirm the hypothesis of Sung et al. (1995). This mutation extinguishes the activity of the protein by disrupting the GTP-induced conformational transition. The final state is much less populated. Having a normal interaction with GAP (Sung et al., 1995) the GTP would be rapidly hydrolyzed and no transforming activity would be observed.

Table 4. *Thermodynamic parameters of the individual steps of BeF_3^- binding to the switch II region mutants Ha-ras-p21*

	Y32W[a]	Y32W-A59T	Y32W-G60A	Y32W-Q61H	Y32W-G75V
ΔH_1^0 (kJ mol^{-1})	15 ± 2	24 ± 5	34 ± 4	11 ± 3	5 ± 4
ΔH_2^0 (kJ mol^{-1})	8 ± 3	16 ± 5	1 ± 1	0 ± 3	−2 ± 1
ΔH_{ov}^0 (kJ mol^{-1})	23 ± 4	40 ± 8	35 ± 4	11 ± 5	3 ± 4
ΔS_1^0 (J mol^{-1} K^{-1})	78 ± 15	110 ± 16	150 ± 14	66 ± 11	44 ± 8
ΔS_2^0 (J mol^{-1} K^{-1})	38 ± 17	49 ± 17	0 ± 5	4 ± 10	−6 ± 4
ΔS_{ov}^0 (J mol^{-1} K^{-1})	111 ± 19	159 ± 24	150 ± 14	70 ± 13	38 ± 13

[a]Data from Díaz et al. (1997a).

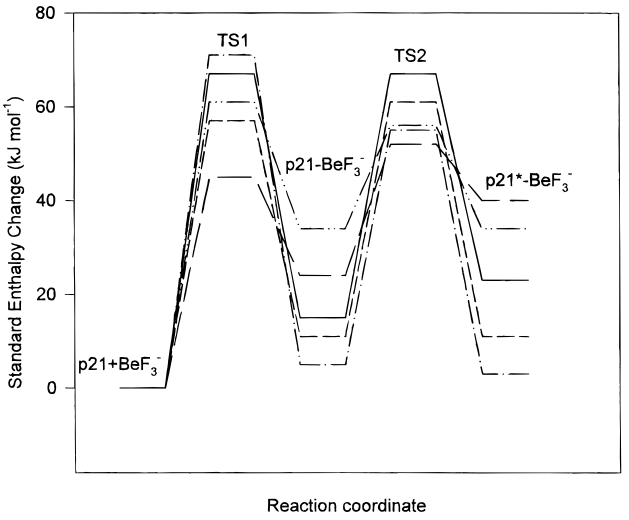

Fig. 5. Standard enthalpy change during the pathway of binding of BeF_3^- to the switch II region mutants. The reference state is the nonassociated mixture of the protein and the complex. TS1 represents the transition state of the BeF_3^- binding while TS2 represents the transition state of the conformational transition. Data for: Solid line Y32W (solid line), Y32W-A59T (long dash), Y32W-G60A (dash-dot-dot), Y32W-Q61H (short dash), Y32W-G75V (dash-dot). The free energy of all the ground states is taken as reference and therefore arbitrarily put to zero. This does not mean that its values is actually zero or identical.

The same effect on the equilibrium constant is observed for the transforming Y32W-A59T mutant. The reason for this should be the phosphorylation of this residue in the transforming protein, causing the γ-phosphate to remain in its site, and leaving the protein in an active state.

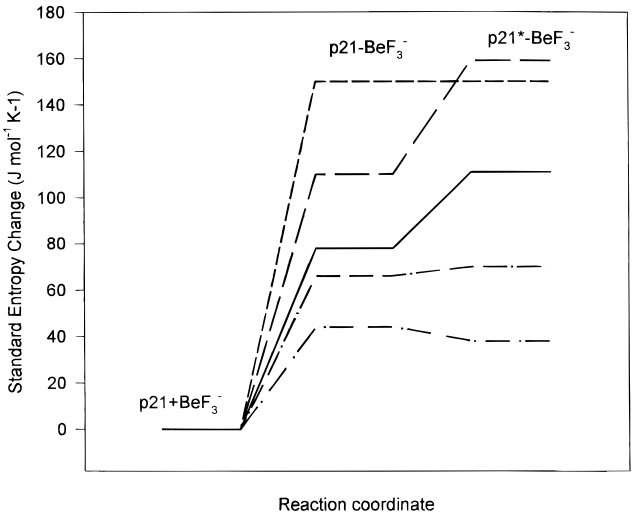

Fig. 6. Standard entropy change during the pathway of binding of BeF_3^- to the switch II region mutants. The reference state is the nonassociated mixture of the protein and the complex. Data for: Y32W (solid line), Y32W-A59T (long dash), Y32W-G60A (short dash), Y32W-Q61H (dash-dot), Y32W-G75V (dash-dot-dot). The standard entropy of all the ground states is taken as reference and therefore arbitrarily put to zero. This does not mean that its value is actually zero or identical.

Gly75 was selected to be mutated since dihedral transitions in this residue are only observed in the early and late states of the conformational transition. This is the only mutation that slows down significantly (a factor of two) the kinetic rate of binding of the analog to its site. This effect is caused by a small increase in the activation energy of the transition. The presence of the side chain contributes to the enthalpy of stabilization of the intermediate state. But contrary to the mutants A59T and G60A, mutation of the side chain at position 75 (G75V) seems to reduce the degrees of freedom, disfavoring the binding reaction entropically. In fact, this mutant has the lowest binding constant of BeF_3^-.

In the second part of the reaction, the conformational transition is affected as well, in a very similar way as for the mutants A59T and G60A; however, no or very weak effect on the activation energy is observed, showing that the interactions with the γ-phosphate (unaffected in this case) are more important for the stability of the transition state. The effect observed is a weak entropic contribution that can be assigned to the loss of conformational freedom of the large side chain during the dihedral switch attributed to the transition state II. The effect is nevertheless much smaller that the one observed for the other two mutants.

Conclusion

The results of the analysis show that the switch II region is involved in both the early and the late states of the conformational transition. The residues that were predicted to alter the pathway of the conformational transition do modify the characteristics of the binding reaction. The control mutant Y32W-Q61H behaves as the reference one, thus giving experimental support to the proposed dynamical pathway (Díaz et al., 1997a) and to the method of targeted molecular dynamics (Schlitter et al., 1994).

Materials and methods

Analytical grade beryllium sulfate and potassium fluoride from Merck (Darmstadt, Germany) were used to prepare the stock solution of beryllium fluoride. All other chemicals employed were analytical grade or better.

The beryllium fluoride stock solution was prepared in buffer A (64 mM Tris, 50 mM HCl, 1 mM NaN_3, 1 mM dithioerythritol (DTE)), containing 1 mM $MgCl_2$, 0.75 M KF and 0.25 M $BeSO_4$; the pH was later adjusted to 7.2. The effective concentration of beryllium trifluoride was calculated using the effective complexing constants of the fluoride beryllium system at a given final concentration of the Be^{2+} and F^- ions (Mesmer & Baes, 1969); the beryllium fluoride concentration of the stock turned out to be 176 mM.

The four double mutants (Y32W-A59T, Y32W-G60A, Y32W-Q61H, and Y32W-G75V) were constructed by long-range PCR (Cheng et al., 1994) of the ptac-*ras* plasmid (Tucker et al., 1986) containing the Y32W mutation that was kindly provided by Dr. A. Wittinghofer. *Escherichia coli* cells of the WK6 line (Δ(lac-proAB) galE straA nal^r [F′ $lacI^q$ lacZΔM15 pro AB^+]) (Zell & Fritz, 1987) were transformed with the obtained plasmids. The mutant proteins were purified as described previously (Díaz et al., 1997a), their purity was checked by SDS-PAGE (Laëmmli, 1970), and their activity was tested by measuring their ability to bind GDP. By scanning the SDS-PAGE gels, it became clear that the prepared proteins were 99% pure, except for the Y32W-A59T

mutant protein that had a purity of 96%. These small impurities did not influence the measurements.

The binding constants of beryllium trifluoride to the mutant proteins were measured in buffer A, 1 mM $MgCl_2$, 1 μM free GDP, pH 7.2, using the change in the fluorescent properties of the tryptophan in the effector loop upon binding of the complex (Díaz et al., 1997a). The fluorimeter used was a Fluorolog 1691 (Spex Industries, Edison, New York). The excitation wavelength was 280 nm, the emission wavelength was 343 nm both with slit apertures of 2 mm, giving a dispersion of 7.2 and 3.6 nm/mm, respectively, for the excitation and emission monochromators. The corrected fluorescence intensity was fitted to Equation 1.

The kinetics of binding of BeF_3^- to both mutants of Ha-*ras*-p21 were measured in buffer A, 1 mM MgCl2, 1 μM GDP, pH 7.2 containing different concentrations of BeF_3^- as described previously (Díaz et al., 1997a). The kinetic constants at a given temperature were obtained by fitting the whole set of curves at different concentrations of BeF_3^- with the programs KINSIM and FITSIM (Barshop et al., 1983), in which the reaction model is programmed. The calculations were performed with a Silicon Graphics Indy workstation (Silicon Graphics Computer Systems, Mountain View, California). This kind of global analysis accounts for the amplitudes of the fast and slow phases, while the graphical analysis of the dependence of the kinetic constants on the concentration of the ligand only uses the information coming from the observed rate constants. The graphical analysis of the molecular structures of the wild-type and the mutants was performed using the WHATIF software package (Vriend, 1990).

Acknowledgments

We thank Dr. Alfred Wittinghofer for the plasmid containing the wild-type (Y32W expression system). Dr. Guido Volkaert for providing laboratory support for the construction and expression of the mutants. Dr. Johan Robben for useful help and suggestions. Mrs. Rosa Martínez-Dalmau for helping with processing the stopped-flow data. This work is supported by Grant OT/97/19 from the Research council of the Katholieke Universiteit Leuven and by Grant 2.0163.94 from the Fund for scientific research (Flanders). J.F.D. was a postdoctoral fellow of the Fund for scientific research (Flanders).

References

Adari H, Lowy DR, Willumsen BM, Der CJ, McCormick F. 1988. Guanosine triphosphatase activating protein (GAP) interacts with the *ras*-p21 effector binding domain. *Science 240*:518–521.

Antonny B, Chardin P, Roux M, Chabre M. 1991. GTP hydrolysis mechanisms in *ras* p21 and in the *ras*-GAP complex studied by fluorescence measurements on tryptophan mutants. *Biochem 30*:8287–8295.

Barbacid M. 1987. *ras* Genes. *Annu Rev Biochem 56*:779–827.

Barshop BA, Wrenn RF, Frieden C. 1983. Analysis of numerical methods for computer simulation of kinetic processes: Development of KINSIM—A flexible, portable system. *Anal Biochem 130*:134–145.

Bigay J, Deterre T, Pfister C, Chabre M. 1987. Fluoride complexes of aluminium or beryllium act on G-proteins as reversibly bound analogues of the γ phosphate of GTP. *EMBO J 6*:2907–2913.

Cheng S, Chang SY, Gravitt P, Respess R. 1994. Long PCR. *Nature 369*:684–685.

Díaz JF, Sillen A, Engelborghs Y. 1997a. Equilibrium and kinetic study of the conformational transition toward the active state of $p21^{Ha\text{-}ras}$, induced by the binding of BeF_3^- to the GDP-bound state, in the absence of GTPase-activating proteins. *J Biol Chem 227*:23138–23143.

Díaz JF, Valpuesta JM, Chacón P, Diakun G, Andreu JM. 1998. Changes in microtubule protofilament number induced by Taxol binding to an easily accessible site. Internal microtubule dynamics. *J Biol Chem 273*:33803–33810.

Díaz JF, Wroblowski B, Engelborghs Y. 1995. Molecular dynamics simulation of the solution structures of *ras*-p21 GDP and GTP complexes. Flexibility, possible hinges, and levers of the conformational transition. *Biochem 34*:12037–12047.

Díaz JF, Wroblowski B, Schlitter J, Engelborghs Y. 1997b. Calculation of pathways for the conformational transition between the GTP- and GDP-bound states of the Ha-*ras*-p21 protein: Calculations with explicit solvent simulations and comparison with calculations in vacuum. *Proteins Struct Funct Genet 28*:434–451.

Kahn RA. 1991. Fluoride is not an activator of the smaller (20–25 kDa) GTP-binding proteins. *J Biol Chem 226*:15595–15597.

Krengel U, Schlichting I, Scherer A, Schumann R, Frech M, John J, Kabsch W, Pai EF, Wittinghofer A. 1990. Three dimensional structure of H-*ras*-p21 mutants: Molecular basis for their inability to function as signal switch molecules. *Cell 62*:539–548.

Kuppens S, Díaz JF, Engelborghs Y. 1999. Characterization of the hinges of the effector loop in the reaction pathway of the activation of *ras*-proteins. Kinetics of binding of beryllium trifluoride to V29G and I36G mutants of Ha-*ras*-p21. *Protein Sci 8*:1860–1866.

Laëmmli UK. 1970. Cleavage of structural proteins during the assembly of the head of bacteriophage T4. *Nature 227*:680–685.

Löwe J, Amos LA. 1998. Crystal structure of the bacterial cell-division protein FtsZ. *Nature 391*:203–206.

Lowy DR, Willumsen BM. 1993. Function and regulation of *ras*. *Annu Rev Biochem 62*:851–891.

McCormick F. 1994. Activators and effectors of *ras* p21 proteins. *Curr Opin Genet Dev 4*:71–76.

Mesmer RE, Baes CF. 1969. Fluoride complexes of beryllium(II) in aqueous media. *Inorg Chem 8*:618–626.

Moore KJM, Webb MR, Eccleston JF. 1993. Mechanism of GTP hydrolysis by $p21^{N\text{-}ras}$ catalysed by GAP: Studies with a fluorescent GTP analogue. *Biochem 32*:7451–7459.

Neal SE, Eccleston JF, Webb MR. 1990. Hydrolysis of GTP by $p21^{NRAS}$, the *NRAS* protooncogene product, is accompanied by a conformational change in the wild-type protein: Use of a single fluorescent probe at the catalytic site. *Proc Natl Acad Sci USA 87*:3562–3565.

Nogales E, Wolf SG, Downing KH. 1998. Structure of $\alpha\beta$-tubulin dimer by electron crystallography. *Nature 391*:199–203.

Pai EF, Krengel U, Petsko GA, Goody RS, Kabsh W, Wittinghofer A. 1990. Refined crystal structure of the triphosphate conformation of H-*ras*-p21 at 1.35 Å resolution: Implications for the mechanism of GTP hydrolysis. *EMBO J 9*:2351–2359.

Schlichting I, Almo SC, Rapp G, Wilson K, Petratos K, Lentfer A, Wittinghofer A, Kabsch W, Pai EF, Petsko GA, et al. 1990. Time-resolved X-ray crystallographic study of the conformational change in Ha-*Ras* p21 protein on GTP hydrolysis. *Nature 345*:309–315.

Schlitter J, Engels M, Krüger P, Jacoby E, Wollmer A. 1994. Targeted molecular dynamics: A new approach for searching pathways of conformational transitions. *J Mol Graphics 12*:84–89.

Sprang SR. 1997. G-protein mechanisms: Insights from structural analysis. *Annu Rev Biochem 66*:639–678.

Sung YJ, Carter M, Zhong JM, Hwang YW. 1995. Mutagenesis of the Ha-*ras*-p21 at glycine-60 residue disrupts GTP-induced conformational change. *Biochemistry 34*:3470–3477.

Tong LA, De Vos AM, Milburn MV, Kim SH. 1991. Crystal structures at 2.2 Å resolution of the catalytic domains of normal *ras* protein and an oncogenic mutant complexed with GDP. *J Mol Biol 217*:503–516.

Tong LA, Milburn MV, De Vos AM, Kim SH. 1989. Structure of *ras*-protein. *Science 245*:244.

Tucker J, Sczakiel G, Feuerstein J, John J, Goody RS, Wittinghofer A. 1986. Expression of p21 proteins in *Escherichia coli* and stereochemistry of the nucleotide-binding site. *EMBO J 5*:1351–1358.

Vriend G. 1990. WHATIF: A molecular modelling and drug design program. *J Mol Graphics 8*:52–56.

Zell R, Fritz HJ. 1987. DNA mismatch-repair in *Escherichia coli* counteracting the hydrolytic deamination of 5-methyl-cytosine residues. *EMBO J 6*:1809–1815.